Image-guided radiotherapy for prostate cancer

Audrey Dang, Patrick A. Kupelian, Minsong Cao, Nzhde Agazaryan, Amar U. Kishan

Department of Radiation Oncology, David Geffen School of Medicine, University of California, Los Angeles, California, USA

Contributions: (I) Conception and design: A Dang, PA Kupelian, AU Kishan; (II) Administrative support: None; (III) Provision of study material or patients: None; (IV) Collection and assembly of data: None; (V) Data analysis and interpretation: None; (VI) Manuscript writing: All authors; (VII) Final approval of manuscript: All authors.

Correspondence to: Amar U. Kishan. Department of Radiation Oncology, David Geffen School of Medicine at UCLA, 200 UCLA Medical Plaza, Suite B265, Los Angeles, CA 90095, USA. Email: aukishan@mednet.ucla.edu.

Abstract: Intensity-modulated radiotherapy (IMRT) has become the standard radiotherapy technology utilized for the treatment of prostate cancer, as it permits the delivery of highly conformal radiation dose distributions. Image-guided radiotherapy (IGRT) is an essential companion to IMRT that allows the treatment team to account for daily changes in target anatomy and positioning. In the present review, we will discuss the different sources of geometric uncertainty and review the rationale behind using IGRT in the treatment of prostate cancer. We will then describe commonly employed IGRT techniques and review their benefits and drawbacks. Additionally, we will review the evidence suggesting a potential clinical benefit to utilizing IGRT.

Keywords: Prostate cancer; image-guided radiotherapy technology (IGRT); intensity-modulated radiation therapy (IMRT); stereotactic body radiotherapy (SBRT); ultrasound (US); cone beam computed tomography (CBCT); electromagnetic transponders; Calypso 4D; cine magnetic resonance imaging (cine MRI); ViewRay; magnetic resonance imaging-guidance (MRI-guidance); stereoscopic X-ray imaging; intraprostatic fiducial markers (FM)

Introduction

Prostate cancer (PCa) is the most common non-cutaneous malignancy in males, with a projected 161,360 incident cases and 26,730 deaths estimated in the United States in 2017 alone (1). Curative modalities for localized PCa include surgery and/or radiation therapy (RT), with or without androgen deprivation therapy. Advances in RT planning and delivery have made it possible to create highly conformal radiation dose distributions by utilizing intensity-modulated radiotherapy (IMRT). As a result of its clear dosimetric benefits over three dimensional conformal radiotherapies (3D-CRT), which imply a potential toxicity benefit, IMRT has quickly become the most common form of RT delivery for PCa (2-4). Extremely hypofractionated treatment regimens, such as stereotactic body radiotherapy (SBRT) regimens, harness the conformality of IMRT and/ or other advanced delivery platforms to deliver RT with

very high degrees of conformality (5-13). The biological effective doses delivered in hypofractionated may be higher for normal tissues and/or tumors due to the larger doses-per-fraction involved; this may be particularly true for PCa, which is thought to be relatively more sensitive to high doses per fraction than normal tissues (14,15).

A consequence of modern, high-conformality RT, however, is the risk of a "geographic miss", which is a well-documented phenomenon (16). Sources of geometric uncertainty include target delineation error, patient setup uncertainty and target position variation (both day-to-day interfraction motion and intrafraction movement during the course of treatment delivery). Image-guided RT (IGRT) allows for the adjustment of patient daily set up as well as the positional correction of the radiation beams during radiation delivery. Failure to account for variations of the prostate gland position as a factor of the deformability and mobility of the surrounding normal gastrointestinal

and genitourinary organs during the course of RT may compromise the control rate and lead to increases in normal tissue toxicity (17). Additionally, the use of IGRT allows for the reduction of planning margins. Thus, IGRT is considered an essential tool in ensuring the safe clinical application of the modern RT techniques.

In this review, we will discuss the different sources of geometric uncertainty that necessitate IGRT and provide a detailed overview of the various IGRT modalities that are being utilized or being actively studied.

Geometric uncertainty

The fundamental sources of geometric uncertainty in RT planning and delivery are errors in target delineation, patient setup uncertainty, interfraction motion and intrafraction motion. Furthermore, errors can also be classified as either systematic or random error. A systematic error is a treatment preparation error and is introduced during the process of planning (i.e., positioning, simulation, or target delineation). A random error is a treatment execution error and varies with each fraction due to its unpredictable nature (18). Systematic errors shift the entire dose distribution away from the clinical target volume (CTV), while random errors blur this distribution around the CTV. A systematic error would affect all treatment fractions uniformly.

Target delineating error relates to the uncertainty during target volume contouring. This depends on both quality of the source imaging modality and interobserver/intraobserver variability in target definition. These errors tend to have a large impact on the dose to the tumor and the surrounding structures that will remain constant during the course of RT; however, IGRT cannot remedy these errors. Computed tomography (CT)-based imaging is the primary source imaging modality for radiation target volume delineation and has relatively poor discrimination of the prostate gland (17). The majority of contouring errors on CT occur at the apex and the base of the prostate gland, in which observers tend to adapt a practice of overestimation of the target contour in order to avoid marginal misses (19-21). Magnetic resonance imaging (MRI) provides better definition of the prostate gland and the surrounding tissues compared with the CT counterpart (22). However, inclusion of MRI information in the treatment planning process requires registration of the MRI volumes to the CT, which in and of itself introduces potential errors in the process of image fusion itself (23).

A second source of geometric uncertainty lies in the daily set up error of the patient. This type of error occurs when the planning anatomical position of the patient is not reproduced at the time of treatment. Immobilization techniques, utilizing either pelvic immobilization only or pelvic and leg immobilization with an alpha cradle system, have been examined to improve the day-to-day reproducibility of treatment setup to the skeletal anatomy (17). Pelvic only immobilization can significantly reduce daily setup variations (from 3–6 mm without immobilization, to 1–3 mm with immobilization) (24-27). Moreover, the addition of leg immobilization was reported to improve both the accuracy and reproducibility of treatment position with reductions in posterior-anterior shifts (2.6 *vs.* 4.4 mm), left-right shifts (2.4 *vs.* 3.6 mm), and cranio-caudal shifts (2.7 *vs.* 3.3 mm) (28). However, the topic of the optimal immobilization device remains controversial, and a full discussion is beyond the scope of this review

Finally, an additional source of geometric uncertainty is the target position variation, both in terms of day-to-day interfraction motion and intrafraction movement during the course of treatment delivery. This error is independent of the bony pelvis positioning—it is a result of the variations in the position, shape, and size of the internal target organs. Previous studies have shown that the bladder and rectal physiology and breathing motion can lead to variability of the prostate's position, however positional changes have been noted to be most markedly correlated with rectal filling (17,29-31). Crook *et al.* reported the average interfractional deviations due to positional variability are typically within 5 mm of the initial target position, though deviations of >10 mm have been observed in up to 30% of cases with maximal deviations of 18 mm (32). Both interfraction and intrafraction uncertainties are a result of a combination of systemic and random errors.

Intrafraction motion characterizes the positional variability of the target during the delivery of the radiation treatment fraction itself. Due to the large amount of dose to be delivered during SBRT treatment that extend the treatment delivery time to 10–20 minutes, the effect of intrafraction motion becomes more important. Intrafraction prostate motion appears to be driven primarily by rectal peristalsis and to a lesser degree with respiratory patterns and variation in pelvic muscular tension. The most significant predictor for intrafraction prostate motion is the status of rectal filling; a more distended rectum could result in greater prostate motion. The effect of respiratory pattern

on intrafraction motion is minimized when the patient is comfortable and in the supine position, as opposed to in the prone position or breathing deeply (29). Using an electromagnetic tracking system, Kupelian *et al.* reported displacements of ≥3 or ≥5 mm for cumulative durations of at least 30 s in 41% and 15% of sessions. Up to 56% of fractions in any given patient showed displacements ≥5 mm (33). Using cine-MRI, studies have reported on prostate displacements of 0.26±3.3 and 0.02±3.6 mm (mean ± SD) in the anterior-posterior (AP) and superior-inferior (SI) dimensions respectively, with maximal displacements up to 1.2 cm anteriorly and superiorly (34). Subsequently, another study reported AP displacements of >5 mm in 29% of patients (35).

van Herk *et al.* has previously defined the planning target volume (PTV) as "*the volume, defined in treatment room coordinates, to which the prescribed dose must be delivered in order to obtain a clinically acceptable and specified probability that the prescribed dose is actually received by the CTV, which has an uncertain location*" and has proposed a model to calculate the ideal PTV margins (36,37). In short, the PTV is a geometric expansion around the CTV, is intended in part to compensate for the above mentioned positional variability. PTV margins were previously generous on the order of 10–15 mm to account for unmeasured prostate motion (38-41). However, the increase in margin comes at an increased toxicity cost to the normal surrounding tissues. Since toxicity is intimately associated with the volume of normal tissue receiving high doses, the use of IGRT offers the opportunity to improve the therapeutic index of prostate RT while reducing toxicity by reducing the PTV margin in a safe manner.

Interfraction motion from daily setup variation has been addressed by ultrasound (US), kilovoltage (kV) or megavoltage (MV) X-ray imaging using implanted fiducial markers (FM), and cone beam computed tomography (CBCT). Technologies such as Calypso® 4D Localization System™ (Calypso Medical, Seattle, WA, USA) and cine MRI (ViewRay®, Cleveland, OH, USA) have been used to monitor intrafraction motion of the prostate (42).

Techniques

Treatment accuracy has significantly improved allowing for both treatment margin optimization and dose escalation due to the implementation of a wide variety of IGRT techniques. These techniques range from daily soft tissue imaging to daily imaging of the implanted FMs. Imaging

methods may broadly be divided into radiation-based and non-radiation-based systems. Non-radiation-based systems include ultrasound, electromagnetic tracking, and MRI systems integrated into the treatment room or treatment machine. Radiation-based IGRT systems include static as well as real time tracking, using either kV, MV, or hybrid methods (18).

CBCT provides excellent spatial resolution for daily positioning; it is also useful in identifying anatomical changes concerning the target volume and organs-at-risk between treatment fractions. CBCT provides a detailed snapshot of the anatomy prior to treatment, but due to the length of image acquisition, this technique is not practical to be used for intrafraction motion management. In contrast, implanted electromagnetic transponders (Calypso® 4D Localization System™), provide superior temporal resolution (and therefore are more useful for monitoring intrafraction motion) but do not provide any information about prostate deformation, seminal vesicle motion, or critical normal tissue motion and deformation (17). MRI-guided RT is able to provide both a detailed snapshot of the anatomy prior to treatment and able to track the target during the treatment as well (43). Although modern localization modalities have significant advantages, they should not be relied upon to overcome poor simulation technique as the goal of simulation is to replicate the conditions that will be used during therapy. For example, significant rectal distension on the initial planning CT is often a compelling indication of prostate deformation and rotation about its typical configuration, and effort should be made to minimize rectal distention (44). The various IGRT methods are reviewed in more detail below. IGRT techniques for proton beam RT are beyond the scope of this review.

Radiopaque intraprostatic markers

There has been an increasing popularity of the use of intraprostatic radiopaque markers with daily in-room imaging as this technique is low cost, is easy to use, and provides limited interobserver variability (45). Three radiopaque markers, such as gold seeds or coils, are implanted into the periphery of the prostate via a transrectal or transperineal approach. Typically, two markers are placed at the posterior base of the prostate and one marker is placed at the apex. The FMs remain stable within the prostate with an average displacement of 1.01–2.8 mm (46-49). On a daily basis, the FMs are visualized with either portal or volumetric imaging and rigid registration by a

radiation therapist is required. When using portal imaging, corrections can be made by matching marker locations to the digitally reconstructed radiographs while with volumetric imaging, a center of mass shift based on the 3-dimensional marker locations is most commonly used, and thus can reduce interobserver variability (50). It appears that the use of multiple FMs (three or more) can help detect rotations. However, only translational shifts can be determined if a single or two FMs are used. Essentially, the markers are a surrogate for the prostate position and thus ensure that the prostate and rectal interface is reproducibly identified even with prostate rotation and deformation. However, the disadvantage is that it requires an invasive procedure that carries the risk of bleeding, infection, and patient discomfort similar to a prostate biopsy. In addition, the markers do not provide information on seminal vesicle localization or changes in the surrounding normal structures overall. However, the dosimetric implications are likely minimal except in rare cases of extreme prostate deformation. The relative importance of prostatic motion with regards to coverage of the nodal volumes in particular has been studied both in the setting of conventional fractionation and SBRT. The use of FMs combined with CBCT for localization results in negligible changes in the dose coverage of pelvic nodes (51,52).

Transabdominal ultrasound

Transabdominal ultrasound-based localization systems use suprapubic transducers to obtain 2-dimensional (2D) or 3-dimensional (3D) images of the target region while the patient is in the treatment position. These images are fused onto the treatment planning CT dataset and a shift correction is calculated in three orthogonal directions to correctly align the prostate with reference to the treatment field isocenter. The entire process including positioning, imaging, and shift correction can be accomplished in 5–7 minutes, and this is performed on a daily basis prior to treatment. This technique has gained widespread popularity in practice due to its low cost and clinical efficiency. However, this technique is operator dependent and thus its accuracy has been questioned (53-56).

van der Meer *et al.* investigated the changes in the internal anatomy using an US-based deformable image registration to create a daily pseudo-CT image compared to the initial simulation CT in three prostate cancer patients. The authors found that the daily pseudo-CT images are more representative of the actual patient anatomy compared to the simulation CT and can reveal changes in tissue distribution that occurred over time. They reported the change in gamma failure for dose (γDose, 3%, 3 mm) ranged from an improvement of 11.2% in the prostate volume to a deterioration of 1.3% in the prostate and bladder. The change in gamma failure for the CT images (γCT, 50 Hounsfield units, 3 mm) ranged from an improvement of 20.5% in the anus and rectum to a deterioration of 3.2% in the prostate (57). The result is compelling, however this study needs to be validated with a larger database.

Furthermore, Krengli *et al.* compared two imaging modalities to verify setup and internal organ variations, utilizing surface imaging by AlignRT® (VisionRT, London, UK) and trans-abdominal US by Clarity (Resonant Medical, Elekta, SE). After adjustment for systematic errors, primarily the uncertainty in the lateral extent of the prostate on ultrasound, the authors noted the setup misalignments between the two imaging modalities were equivalent, in the range from –7 to 7 mm corresponding to the author's institutional PTV margin expansion in the anteroposterior direction (58).

Conversely, studies have compared the differences between marker alignments and US-based guidance. Langen *et al.* found directed differences in the means (± SD) between US and marker alignments of 0.2 (±3.7), 2.7 (±3.9), and 1.6 (±3.1) mm in the AP, SI, and lateral directions (53). Thus, this measurable difference suggests that this technique should be used with caution and its uncertainty in reproducibility should be accounted for with appropriate PTV margins. The uncertainties associated with US have been attributed to image quality, interobserver variability, operator-induced displacement of the prostate by probe pressure, and alignment uncertainty from contour volume differences between daily US and the planning CT. Other factors that could negatively impact image quality include larger body habitus, inadequate bladder filling and shadowing of the prostate by the pubic symphysis which leads to a reliance on the prostate-bladder interface for alignment in the SI axis (17).

Electromagnetic transponders

The Calypso® 4D Localization System™ (Calypso Medical Technologies, Seattle, WA, USA), allows both pretreatment localization of the prostate and real-time evaluation of the intrafraction motion (59). Prior to treatment planning, three small nonradioactive electromagnetic transponders

(or beacons) are implanted into the prostate at the apex and bilateral base of the prostate in a process similar to the placement of the intraprostatic FMs. Each beacon, measuring 8.8 mm long × 1.85 mm in diameter, contains a capacitor and an inductor coil sealed in glass.

The Calypso® 4D Localization System™ consists of a tracking console in the RT control room that interfaces with ceiling mounted infrared cameras located in the treatment vault. These cameras are in turn integrated with an electromagnetic array which is placed over the patient before and during treatment. Using resonant radiofrequencies, the electromagnetic array excites and localizes the beacon transponders that have been implanted in the prostate. During daily radiation treatments, the beacon transponders communicate with the Calypso® 4D Localization System™ using safe radiofrequency wavelengths with real time tracking of their location 10 times per second. Using the camera system, the array determines the location of the prostate which is then aligned to the position of the room and the treatment unit. This system allows real time evaluation of intrafractional prostate motion, to monitor and account for motion during the course of treatment. Additionally, this system can localize the prostate within 1 mm at the start of therapy. In a study of over 1,157 treatment fractions across 35 patients treated at 5 institutions, electromagnetic monitoring and correction studies found that without guidance, margins of over 10 mm were necessary to ensure 95% dosimetric coverage, while with guidance, margins of 2–3 mm were reasonable (60).

Overall, the advantages of this system include lack of ionizing radiation during imaging, real-time tracking to allow for more accurate treatment delivery, adaptive and interactive patient positioning capabilities, and reduced treatment margins to minimize surrounding normal tissue toxicity. However, the disadvantage of this system is strict criteria for patient eligibility, such that patients with hip prostheses or large metal implants in the proximity of the prostate, those with a pacemaker or other implanted electromagnetic devices, and patients with larger body habitus that corresponds to the transponder being >27 cm from the array, cannot be tracked adequately (59,61).

CT-based image guidance

In-room CT systems are classified by the beam quality, MV or kV, and beam collimation, fan-beam or cone-beam. The fan-beam systems use a linear array of detectors in conjunction with a rotating fan beam X-ray source; this system can be integrated with a linear accelerator that generates X-rays for both treatment and imaging or can exist as a peripheral CT-gantry. CBCT systems use an open beam X-ray source and large flat-panel detector mounted on the accelerator gantry perpendicular to the primary treatment axis, thus allowing for an entire image volume to be reconstructed from a single gantry rotation. Varian and Elekta offer gantry-mounted kilovoltage CBCT systems (Elekta Synergy® and Varian On-Board Imager®); in contrast, Siemens offers an integrated megavoltage CBCT system (MVision). Other systems include integrated helical fan-beam megavoltage CT (TomoTherapy®) and peripheral fan-beam kV CT (CT-on-rails™). Compared to MV-imaging, kV-imaging technique is superior due to its enhanced soft-tissue image contrast secondary to the prevalence of photoelectric interactions at low energies; however, this system remains inferior to conventional CT. CT-on-rails™ offers the highest image quality among the available in-room imaging systems. However, the alignment between the CT-on-rails™ and the linear accelerator isocenter does not have the same rigidity as does the alignment offered by other CT-based image-guidance systems since the imaging and treatment equipment do not share a gantry; thus, this system introduces an intrinsic uncertainty of treatment versus imaging isocenter and has mostly been replaced by the onboard imaging systems due to the more user-friendly format of the latter (17,62,63).

CT-based localization methods allow daily visualization of the prostate and enable direct soft tissue alignment. Additionally, CT-based methods can detect interfractional soft tissue changes such as prostate deformation, rectal distension, and bladder filling. This additional anatomic information allows for onboard re-planning and calculation of daily dose volume histograms for both the target and adjacent normal tissues at risk as needed. The disadvantage of CT-based methods remains in the limited resolution of onboard imaging systems which creates a challenge in determining the precise location of the prostate, as well as the image acquisition time, prohibiting its use for intrafraction monitoring. Other alternative techniques include intraprostatic FM alignment, planning CT contour alignment, and automatic 3D gray-value registration are used to enhance onboard CT-based methods. The use of FMs has been shown to significantly reduce the inter-user variability associated with both of the non-marker-based methods (50,64). In a retrospective study, Nakamura *et al.* evaluated the acute toxicity and biochemical tumor control of prostate IMRT using two different IGRT

techniques without intraprostatic FMs, using orthogonal kV radiographs using the ExacTrac® System (BrainLAB AG, Munich, Germany) and CBCT, as bony structure-based IGRT and prostate-based IGRT, respectively. Margins were 1–3 mm smaller in the prostate-based IGRT compared to the bony structure-based IGRT. The authors found a significantly lower incidence of acute grade >2 gastrointestinal toxicities in the prostate-based IGRT and the 3-year biochemical failure-free survival were equivalent between the two groups (65).

Alternatively, the imaging information acquired with CBCT can be used for adaptive radiation therapy (ART) as an off-line correction strategy. ART was first introduced by Yan *et al.* and Martinez *et al.* While a full discussion of ART is beyond the scope of this review, it is a technique wherein imaging information from the first few fractions are utilized to reoptimize the treatment plan and accounting for systematic errors from setup errors and organ motion (66,67). In summary, CT-based image guidance can be used as both off-line and on-line IGRT method.

MRI-guidance

Due to its superior soft-tissue resolution, MRI has emerged as an important imaging modality for target delineation (68). Classically, MRI studies have previously been used to observe prostate motion and have provided information on the frequency and magnitude of intrafraction prostate motion. However, these historical studies have been limited as the prostate was monitored for a relatively short time rather than continuously or was not monitored during radiation treatment (31,34,35,69). Studies with continuous MRI have demonstrated that intrafraction motion of both the prostate and seminal vesicles increases with treatment time. The intrafraction motion of the seminal vesicles does not move in unison with the prostate. Seminal vesicle displacement ranges from 4–7 mm in the AP direction in 15 minutes, 4.7–7.2 mm in the SI direction in 15 minutes, and 2.7–3.4 mm in the left-right direction in 10 minutes. It was also noted that the seminal vesicles move more than the prostate in SI direction, but not in the AP direction. Prostate displacement was <5 mm in all directions (70).

More recently, a study of an open-MRI simulation workflow in ten patients found differences in shift positions for the cohort between CBCT-to-CT registration and CBCT-to-MRI registration, ranging on the order of 0.01–0.25 cm with the highest degree of motion seen in the anteroposterior axis (71). The results underscore the potential benefits of MRI-based contouring and target localization. Indeed, an integrated MRI approach has several putative advantages: (I) it can facilitate more accurate target definition/delineation during contouring; (II) it can achieve direct, individual nodal imaging in the RT position; and (III) 4D MRI facilitates real time imaging. Furthermore, the combination of high soft tissue definition due to MRI and real-time gating without the cost of low dose radiation exposure from X-ray or CT imaging also eliminates the need for FMs. The disadvantages with MRI include motion artifacts, distortion with non-uniform magnetic fields, and inability to be used in patients with pacemakers or metallic implants (18).

With regards to MRI-based radiotherapy itself, there are multiple technical challenges. The presence of a magnetic field can complicate RT delivery due to electromagnetic interference with the linear accelerator and alterations in the planned dose delivery (72). The ViewRay® magnetic resonance (MR) system (ViewRay®, Inc., Cleveland, OH, USA) is the first commercial MR-guided RT system and seeks to mitigate these effects by virtue of employing a low-field magnet and three ^{60}Co sources in place of a linear accelerator (73). This system can facilitate tumor tracking during beam delivery (gating) and also allows for adaptive planning (74-76). Experience utilizing the ViewRay® is increasing, and it is anticipated that the advent of an MRI-LINAC system will further increase the profile of MRI-based IGRT by virtue of offering improved dosimetry. The MRI-LINAC system has been pioneered by the Medical Center Utrecht, the Netherlands, Elekta AB (Stockholm, Sweden), and Philips (Best, the Netherlands) and, the first patient to receive treatment on such a system was treated in May 2017. The potential for this platform is tremendous, and short-term toxicity and efficacy results are eagerly anticipated (77).

Clinical outcomes

The clinical implementation of IGRT has improved treatment accuracy and margin reduction in prostate cancer RT, however it is uncertain whether the dosimetric and geometric gains can actually lead to improved clinical outcomes. To date, no level 1 evidence is available. However, historical data in the pre-IGRT era have demonstrated the clinical impact of anatomic variations. Further, as the majority of the dose-escalation trials that showed improved outcomes relied on portal imaging of bony anatomy for localization, it has been argued that the benefit of dose-escalation may relate to better coverage of

the prostate rather than the higher dose (49,78).

de Crevoisier *et al.* reported on the effect of rectal distension at the time of simulation on biochemical control in 127 prostate cancer patients treated with high dose 3D-CRT. Patients with distended rectums, defined as a cross sectional area (CSA) >11.2 cm^2, on the planning CT scan had a 29% decrease in biochemical control at 5 years (63% for CSA >11.2 cm^2 and 92% for CSA <11.2 cm^2) (79). Heemsbergen *et al.* validated this observation in patients treated without image guidance on the Dutch randomized dose-escalation study (80). The increase in biochemical failure in these studies was suspected to be due to possible geographic misses secondary to systematic error involving the posterior displacement of the prostate during treatment relative to its position at the time of planning. In a retrospective study, Kupelian *et al.* evaluated the impact of rectal distension in 488 patients treated with daily transabdominal ultrasound guidance. The use of daily image guidance eliminated error such as rectal distension at the time of simulation (81). Furthermore, Raziee *et al.* reported an improvement in disease-specific outcomes in 961 patients treated with progressive dose escalation using IGRT with three sequential institutional schedules: (I) 75.6 Gy (3D-CRT); (II) 79.8 Gy (IMRT); and (III) 78 Gy (VMAT). The 5-year biochemical recurrence rates in cohorts A, B and C were 23%, 17% and 9%, respectively. However, metastasis incidence, cause-specific death and toxicities were not different between the three cohorts (78).

Singh *et al.* evaluated the post-treatment patient-reported quality of life (QOL) of 282 prostate cancer patients after being treated with (n=154) and without (n=128) IGRT, using FMs and MR prostatic image fusion with FMs *in situ*. Improvement was noted in all dysfunctional rectal symptoms in the IGRT cohort. Additionally, IGRT improved rectal pain, urgency, diarrhea, and change in bowel habits. There was also a significant reduction of bowel dysfunctional symptoms in the IGRT cohort, even though this group had larger volumes of rectum treated to higher doses (82). In another prospective study, Gill *et al.* reported a significant improvement in acute treatment-related toxicity, according to Common Terminology Criteria Adverse Events V3.0, with the implementation of IGRT (n=249) and dose escalation up to 78 Gy in 39 fractions compared to the cohort without IGRT (n=26). The authors reported statistically significant improvements in the multiple acute toxicity domains with non-IGRT *vs.* IGRT: grade >3 urinary frequency (23% *vs.* 7%); grade >2 diarrhea (15% *vs.* 3%); and grade >2 fatigue (23% *vs.* 8%) (83).

Perhaps the most significant data supporting IGRT were provided by Zelefsky *et al.* (84). The investigators compared clinical outcomes between 186 patients treated with IGRT (in this case, fiducials) to 86.4 Gy with the outcomes of 190 patients treated to the same dose without IGRT. With a median follow-up of 2.8 years, a significant reduction in late urinary toxicity was found with IGRT, with a grade ≥2 genitourinary toxicity rate of 20% *vs.* 10%, respectively, without and with IGRT. The incidence of grade ≥2 gastrointestinal toxicity was similar in both cohorts. In the high-risk group, a significant biochemical control benefit to IGRT was found.

The multi-institutional AIM trial (Assessing the Impact of Margin Reduction) was the first prospective study to report a decrease in the acute reduction in patient reported QOL outcomes in patients treated with a reduced PTV margin (3 mm) using IMRT and electromagnetic tracking to deliver 81 Gy (85). QOL data was obtained prior to and after the completion of treatment and compared to the PROST-QA results (86). For the PROST-QA group, IMRT was used with conventional PTV margins of 5 to 10 mm to deliver radiation doses of 75.6 to 79.2 Gy. AIM study patients experienced meaningful decline in only one health-related QOL domain (urinary) and experienced significantly less toxicity in the bowel/rectal, urinary obstructive and urinary incontinence domains as compared to PROST-QA group (85). A reduction in acute treatment related toxicity is of particular importance, since evidence suggests that patients who exhibit acute toxicity are seven times more likely to develop late toxicity (87).

In summary, IGRT techniques appear to be associated with an improved toxicity profile (particularly improved genitourinary toxicity) and improved treatment efficacy. IGRT allows for margin reduction as well, and imbues greater confidence in highly conformal treatments. Newer strategies, such as kilovoltage intrafraction monitoring (88), constitute exciting venues of further study.

Sample protocol

At our institution, SBRT is routinely offered to patients with low- or intermediate-risk PCa using linear accelerator-based volumetric-modulated arc therapy to deliver 40 Gy in 5 fractions to the prostate PTV. CT simulation scans are performed in the supine position, without contrast and with 1.5 mm slice thickness. We utilize a bladder-filling protocol in order to maximize reproducibility of bladder distention at the time of simulation and subsequent treatment fractions.
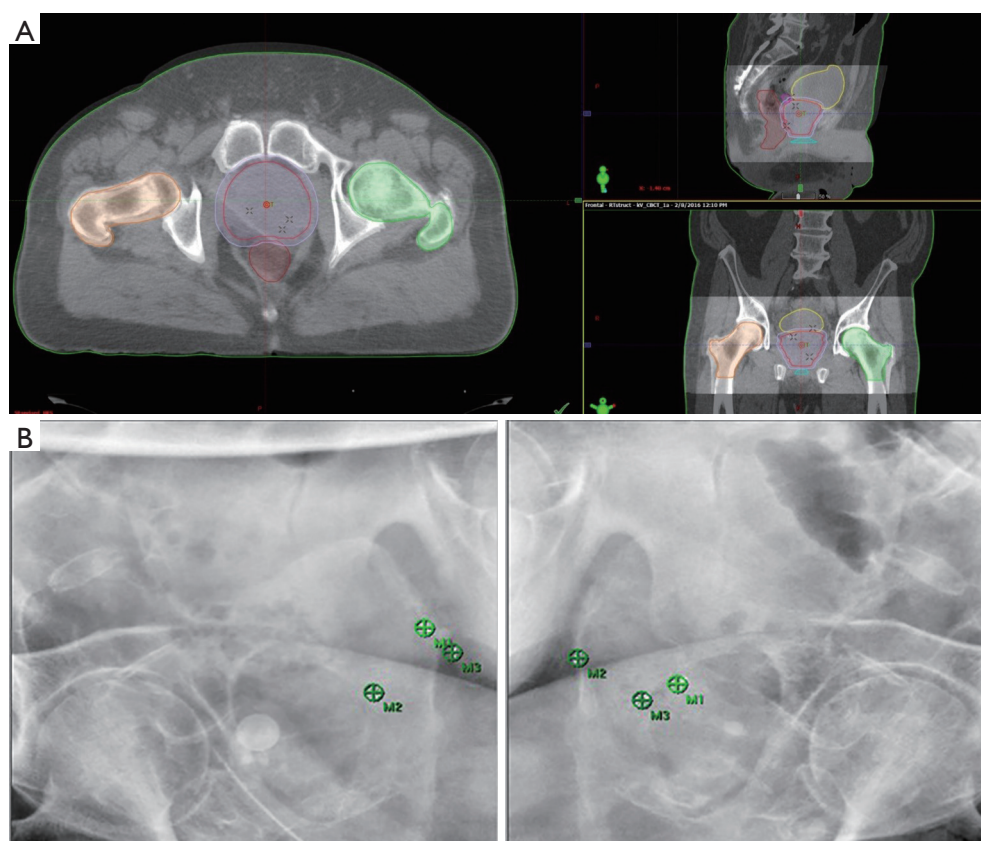
Figure 1 IGRT consisting of CBCT (A) and stereoscopic X-ray imaging (B) with ExacTrac® at setup are used at every treatment fraction to verify the internal anatomy and intraprostatic fiducial markers. Bladder filling and the extent of rectal distension are rigorously scrutinized at the time of simulation and each treatment fraction by the attending radiation oncologist. IGRT, image-guided radiotherapy; CBCT, cone beam computed tomography.

Patients are instructed to void one hour before simulation and treatment, and then drink 16 oz of water. A specific bowel protocol is not utilized. However, we routinely closely scrutinize the degree of rectal distension at the time of simulation and treatment.

At the time of treatment, the initial patient positioning is accomplished using cone beam CT and stereoscopic X-ray imaging with ExacTrac® (BrainLAB AG, Munich, Germany), with the attending radiation oncologist acceptance of anatomy at each fraction, followed by stereoscopic alignment of intraprostatic FMs. Volumetric-modulated arc therapy using four half arcs and 6 MV photons is generally used for treatment delivery with stereoscopic imaging performed before each half arc. Please see *Figure 1* for a sample of our current imaging protocol and *Figure 2* for our institutional IGRT and treatment delivery work flow. The overall treatment time generally takes 10 minutes or less, and

treatment is delivered every other day.

For standard fractionation treatment of PCa, our institution implements daily stereoscopic X-ray imaging with ExacTrac® followed by stereoscopic alignment of intraprostatic FMs. CBCT is used once a week to verify the internal anatomy as well.

Conclusions

The definitive treatment of prostate cancer with external beam RT has drastically improved in the past score with modern techniques such as IMRT or SBRT. The implementation of daily image guidance techniques has helped reduce the impact of prostate motion associated with the positional variability of the prostate. In addition, image guidance has also allowed for a reduction in PTV margin and thus an improved toxicity profile which translates
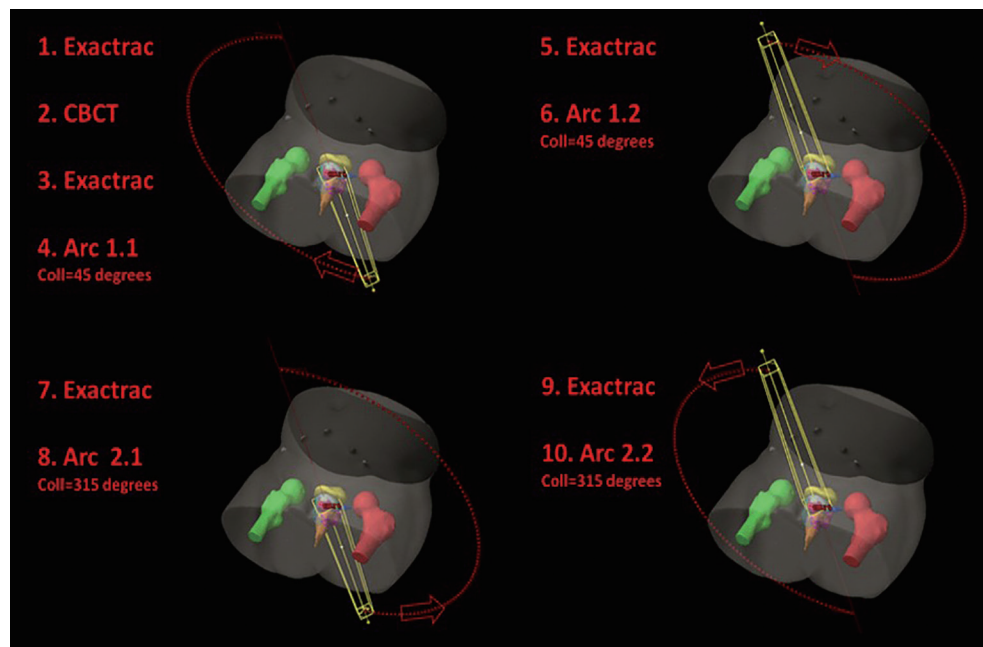
Figure 2 A sample of our institutional IGRT work flow during the treatment of SBRT for prostate cancer. Initially, patient positioning is accomplished by using CBCT and stereoscopic X-ray imaging with ExacTrac®, in which will be verified by the attending radiation oncologist. A repeat stereoscopic X-ray is obtained prior to each half arc treatment delivery in order to ensure that no movement has occurred during the process of IGRT and treatment delivery. IGRT, image-guided radiotherapy; CBCT, cone beam computed tomography; SBRT, stereotactic body radiotherapy.

to an improved patient-reported QOL. Targeting the prostate utilizing FMs, X-ray, CT scans, and ultrasound allows management of interfraction set up variability. Meanwhile, MRI-guidance allows for both interfraction and intrafraction motion management. The role of IGRT has increased in importance as studies have shown a benefit in dose escalation while balancing the toxicity profile is just as crucial in clinical practice.

Acknowledgements

None.

Footnote

Conflicts of Interest: The authors have no conflicts of interest to declare.

References

1. Cancer Stat Facts: Prostate Cancer. Bethesda, MD: National Cancer Institute, 2017. Available online: https:// seer.cancer.gov/statfacts/html/prost.html

2. Lee I, Sandler HA. Hormone therapy and radiotherapy for intermediate risk prostate cancer. Semin Radiat Oncol 2008;18:7-14.

3. Osman SO, Jeevanandam P, Kanakavelu N, et al. Class solutions for SABR-VMAT for high-risk prostate cancer with and without elective nodal irradiation. Radiat Oncol 2016;11:155.

4. Yu T, Zhang Q, Zheng T, et al. The Effectiveness of Intensity Modulated Radiation Therapy versus Three-Dimensional Radiation Therapy in Prostate Cancer: A Meta-Analysis of the Literatures. PLoS One 2016;11:e0154499.

5. Boike TP, Lotan Y, Cho LC, et al. Phase I dose-escalation study of stereotactic body radiation therapy for low- and intermediate-risk prostate cancer. J Clin Oncol 2011;29:2020-6.

6. Bolzicco G, Favretto MS, Scremin E, et al. Image-guided stereotactic body radiation therapy for clinically localized prostate cancer: preliminary clinical results. Technol Cancer Res Treat 2010;9:473-7.

7. Friedland JL, Freeman DE, Masterson-McGary ME, et

al. Stereotactic body radiotherapy: an emerging treatment approach for localized prostate cancer. Technol Cancer Res Treat 2009;8:387-92.

8. Kim DW, Straka C, Cho LC, et al. Stereotactic Body Radiation Therapy for Prostate Cancer: Review of Experience of a Multicenter Phase I/II Dose-Escalation Study. Front Oncol 2014;4:319.

9. King CR, Brooks JD, Gill H, et al. Long-term outcomes from a prospective trial of stereotactic body radiotherapy for low-risk prostate cancer. Int J Radiat Oncol Biol Phys 2012;82:877-82.

10. King CR, Freeman D, Kaplan I, et al. Stereotactic body radiotherapy for localized prostate cancer: pooled analysis from a multi-institutional consortium of prospective phase II trials. Radiother Oncol 2013;109:217-21.

11. Kishan AU, King CR. Stereotactic Body Radiotherapy for Low- and Intermediate-Risk Prostate Cancer. Semin Radiat Oncol 2017;27:268-78.

12. Madsen BL, Hsi RA, Pham HT, et al. Stereotactic hypofractionated accurate radiotherapy of the prostate (SHARP), 33.5 Gy in five fractions for localized disease: first clinical trial results. Int J Radiat Oncol Biol Phys 2007;67:1099-105.

13. McBride SM, Wong DS, Dombrowski JJ, et al. Hypofractionated stereotactic body radiotherapy in low-risk prostate adenocarcinoma: preliminary results of a multi-institutional phase 1 feasibility trial. Cancer 2012;118:3681-90.

14. Daşu A. Is the alpha/beta value for prostate tumours low enough to be safely used in clinical trials? Clin Oncol (R Coll Radiol) 2007;19:289-301.

15. Fowler JF, Ritter MA, Chappell RJ, et al., What hypofractionated protocols should be tested for prostate cancer? Int J Radiat Oncol Biol Phys 2003;56:1093-104.

16. Bell LJ, Cox J, Eade T, et al. Determining optimal planning target volume and image guidance policy for post-prostatectomy intensity modulated radiotherapy. Radiat Oncol 2015;10:151.

17. Stenmark MH, Hamstra DA. Image-Guided Strategies for Prostate Cancer. In: Thomas CR, editor. Radiation Medicine Rounds Prostate Cancer. Demos Medical Publishing, 2011:113-30.

18. Goyal S, Kataria T. Image guidance in radiation therapy: techniques and applications. Radiol Res Pract 2014;2014:705604.

19. Roach M, Faillace-Akazawa P, Malfatti C, et al. Prostate volumes defined by magnetic resonance imaging and computerized tomographic scans for three-dimensional

conformal radiotherapy. . Int J Radiat Oncol Biol Phys 1996;35:1011-8.

20. Rasch C, Barillot I, Remeijer P, et al. Definition of the prostate in CT and MRI: a multi-observer study. Int J Radiat Oncol Biol Phys 1999;43:57-66.

21. McLaughlin PW, Evans C, Feng M, et al. Radiographic and anatomic basis for prostate contouring errors and methods to improve prostate contouring accuracy. Int J Radiat Oncol Biol Phys 2010;76:369-78.

22. Parker CC, Damyanovich A, Haycocks T, et al. Magnetic resonance imaging in the radiation treatment planning of localized prostate cancer using intra-prostatic fiducial markers for computed tomography co-registration. Radiother Oncol 2003;66:217-24.

23. Roberson PL, McLaughlin PW, Narayana V, et al. Use and uncertainties of mutual information for computed tomography/ magnetic resonance (CT/MR) registration post permanent implant of the prostate. Med Phys 2005;32:473-82.

24. Soffen EM, Hanks GE, Hwang CC, et al. Conformal static field therapy for low volume low grade prostate cancer with rigid immobilization. Int J Radiat Oncol Biol Phys 1991;20:141-6.

25. Rosenthal SA, Roach M 3rd, Goldsmith BJ, et al. Immobilization improves the reproducibility of patient positioning during six-field conformal radiation therapy for prostate carcinoma. Int J Radiat Oncol Biol Phys 1993;27:921-6.

26. Bentel GC, Marks LB, Sherouse GW, et al. The effectiveness of immobilization during prostate irradiation. Int J Radiat Oncol Biol Phys 1995;31:143-8.

27. Rattray G, Hopley S, Mason N, et al. Assessment of pelvic stabilization devices for improved field reproducibility. Australas Radiol 1998;42:118-25.

28. Fiorino C, Reni M, Bolognesi A, et al. Set-up error in supine-positioned patients immobilized with two different modalities during conformal radiotherapy of prostate cancer. Radiother Oncol 1998;49:133-41.

29. Dawson LA, Litzenberg DW, Brock KK, et al. A comparison of ventilatory prostate movement in four treatment positions. Int J Radiat Oncol Biol Phys 2000;48:319-23.

30. Dawson LA, Mah K, Franssen E, et al. Target position variability throughout prostate radiotherapy. Int J Radiat Oncol Biol Phys 1998;42:1155-61.

31. Ghilezan MJ, Jaffray DA, Siewerdsen JH, et al. Prostate gland motion assessed with cine-magnetic resonance imaging (cine-MRI). Int J Radiat Oncol Biol Phys

2005;62:406-17.

32. Crook JM, Raymond Y, Salhani D, et al. Prostate motion during standard radiotherapy as assessed by fiducial markers. Radiother Oncol 1995;37:35-42.

33. Kupelian P, Willoughby TR, Mahadevan A, et al. Multi-institutional clinical experience with the Calypso System in localization and continuous, real-time monitoring of the prostate gland during external radiotherapy. Int J Radiat Oncol Biol Phys 2007;67:1088-98.

34. Mah D, Freedman G, Milestone B, et al. Measurement of intrafractional prostate motion using magnetic resonance imaging. Int J Radiat Oncol Biol Phys 2002;54:568-75.

35. Padhani AR, Khoo VS, Suckling J, et al. Evaluating the effect of rectal distension and rectal movement on prostate gland position using cine MRI. Int J Radiat Oncol Biol Phys 1999;44:525-33.

36. van Herk M. Errors and margins in radiotherapy. Semin Radiat Oncol 2004;14:52-64.

37. van Herk M, Remeijer P, Rasch C, et al. The probability of correct target dosage: dose-population histograms for deriving treatment margins in radiotherapy. Int J Radiat Oncol Biol Phys 2000;47:1121-35.

38. Cahlon O, Hunt M, Zelefsky MJ. Intensity-modulated radiation therapy: supportive data for prostate cancer. Semin Radiat Oncol 2008;18:48-57.

39. Eade TN, Hanlon AL, Horwitz EM, et al. What dose of external-beam radiation is high enough for prostate cancer? Int J Radiat Oncol Biol Phys 2007;68:682-9.

40. Kuban DA, Tucker SL, Dong L, et al. Long-term results of the M. D. Anderson randomized dose-escalation trial for prostate cancer. Int J Radiat Oncol Biol Phys 2008;70:67-74.

41. Zietman AL, DeSilvio ML, Slater JD, et al. Comparison of conventional-dose vs. high-dose conformal radiation therapy in clinically localized adenocarcinoma of the prostate: a randomized controlled trial. JAMA 2005;294:1233-9.

42. Langen KM, Willoughby TR, Meeks SL, et al. Observations on real-time prostate gland motion using electromagnetic tracking. Int J Radiat Oncol Biol Phys 2008;71:1084-90.

43. Arivarasan I, Anuradha C, Subramanian S, et al. Magnetic resonance image guidance in external beam radiation therapy planning and delivery. Jpn J Radiol 2017;35:417-26.

44. Maggio A, Gabriele D, Garibaldi E, et al. Impact of a rectal and bladder preparation protocol on prostate cancer outcome in patients treated with external beam radiotherapy. Strahlenther Onkol 2017;193:722-32.

45. Kudchadker RJ, Lee AK, Yu ZH, et al. Effectiveness of using fewer implanted fiducial markers for prostate target alignment. Int J Radiat Oncol Biol Phys 2009;74:1283-9.

46. Kupelian PA, Willoughby TR, Meeks SL, et al. Intraprostatic fiducials for localization of the prostate gland: monitoring intermarker distances during radiation therapy to test for marker stability. Int J Radiat Oncol Biol Phys 2005;62:1291-6.

47. Poggi MM, Gant DA, Sewchand W, et al. Marker seed migration in prostate localization. Int J Radiat Oncol Biol Phys 2003;56:1248-51.

48. Pouliot J, Aubin M, Langen K, et al. (Non)-migration of radiopaque markers used for on-line localization of the prostate with an electronic portal imaging device. Int J Radiat Oncol Biol Phys 2003;56:862-6.

49. Schallenkamp JM, Herman MG, Kruse JJ, et al. Prostate position relative to pelvic bony anatomy based on intraprostatic gold markers and electronic portal imaging. Int J Radiat Oncol Biol Phys 2005;63:800-11.

50. Moseley DJ, White EA, Wiltshire KL, et al. Comparison of localization performance with implanted fiducial markers and cone-beam computed tomography for on-line image-guided radiotherapy of the prostate. Int J Radiat Oncol Biol Phys 2007;67:942-53.

51. Hsu A, Pawlicki T, Luxton G, et al. A study of image-guided intensity-modulated radiotherapy with fiducials for localized prostate cancer including pelvic lymph nodes. Int J Radiat Oncol Biol Phys 2007;68:898-902.

52. Kishan AU, Lamb JM, Jani SS, et al. Pelvic nodal dosing with registration to the prostate: implications for high-risk prostate cancer patients receiving stereotactic body radiation therapy. Int J Radiat Oncol Biol Phys 2015;91:832-9.

53. Langen KM, Pouliot J, Anezinos C, et al. Evaluation of ultrasound-based prostate localization for image-guided radiotherapy. Int J Radiat Oncol Biol Phys 2003;57:635-44.

54. Lattanzi J, McNeeley S, Pinover W, et al. A comparison of daily CT localization to a daily ultrasound-based system in prostate cancer. Int J Radiat Oncol Biol Phys 1999;43:719-25.

55. McNair HA, Mangar SA, Coffey J, et al. A comparison of CT- and ultrasound-based imaging to localize the prostate for external beam radiotherapy. Int J Radiat Oncol Biol Phys 2006;65:678-87.

56. Scarbrough TJ, Golden NM, Ting JY, et al. Comparison of ultrasound and implanted seed marker prostate localization methods: Implications for image-guided radiotherapy. Int J Radiat Oncol Biol Phys 2006;65:378-87.

57. van der Meer S, Camps SM, van Elmpt WJ, et al. Simulation of pseudo-CT images based on deformable image registration of ultrasound images: A proof of concept for transabdominal ultrasound imaging of the prostate during radiotherapy. Med Phys 2016;43:1913.

58. Krengli M, Loi G, Pisani C, et al. Three-dimensional surface and ultrasound imaging for daily IGRT of prostate cancer. Radiat Oncol 2016;11:159.

59. Willoughby TR, Kupelian PA, Pouliot J et al. Target localization and real-time tracking using the Calypso 4D localization system in patients with localized prostate cancer. Int J Radiat Oncol Biol Phys 2006;65:528-34.

60. Litzenberg DW, Balter JM, Hadley SW, et al. Prostate intrafraction translation margins for real-time monitoring and correction strategies. Prostate Cancer 2012;2012:130579.

61. Balter JM, Wright JN, Newell LJ, et al. Accuracy of a wireless localization system for radiotherapy. Int J Radiat Oncol Biol Phys 2005;61:933-7.

62. Ma CM and Paskalev K. In-room CT techniques for image-guided radiation therapy. Med Dosim 2006;31:30-9.

63. Court L, Rosen I, Mohan R, et al. Evaluation of mechanical precision and alignment uncertainties for an integrated CT/LINAC system. Med Phys 2003;30:1198-210.

64. Langen KM, Zhang Y, Andrews RD, et al. Initial experience with megavoltage (MV) CT guidance for daily prostate alignments. Int J Radiat Oncol Biol Phys 2005;62:1517-24.

65. Nakamura K, Mizowaki T, Inokuchi H, et al. Decreased acute toxicities of intensity-modulated radiation therapy for localized prostate cancer with prostate-based versus bone-based image guidance. Int J Clin Oncol 2018;23:158-64.

66. Martinez AA, Yan D, Lockman D, et al. Improvement in dose escalation using the process of adaptive radiotherapy combined with three-dimensional conformal or intensity-modulated beams for prostate cancer. Int J Radiat Oncol Biol Phys 2001;50:1226-34.

67. Yan D, Lockman D, Brabbins D, et al. An off-line strategy for constructing a patient-specific planning target volume in adaptive treatment process for prostate cancer. Int J Radiat Oncol Biol Phys 2000;48:289-302.

68. Hentschel B, Oehler W, Strauss D, et al. Definition of the CTV prostate in CT and MRI by using CT-MRI image fusion in IMRT planning for prostate cancer. Strahlenther Onkol 2011;187:183-90.

69. Ogino I, Kaneko T, Suzuki R, et al. Rectal content and intrafractional prostate gland motion assessed by magnetic resonance imaging. J Radiat Res 2011;52:199-207.

70. Gill S, Dang K, Fox C, et al. Seminal vesicle intrafraction motion analysed with cinematic magnetic resonance imaging. Radiat Oncol 2014;9:174.

71. Doemer A, Chetty IJ, Glide-Hurst C, et al. Evaluating organ delineation, dose calculation and daily localization in an open-MRI simulation workflow for prostate cancer patients. Radiat Oncol 2015;10:37.

72. Raaijmakers AJ, Raaymakers BW, Lagendijk JJ. Magnetic-field-induced dose effects in MR-guided radiotherapy systems: dependence on the magnetic field strength. Phys Med Biol 2008;53:909-23.

73. Hu Y, Green OP, Parikh P, et al. TH-E-BRA-07: Initial Experience with the ViewRay System - Quality Assurance Testing of the Imaging Component. Medical Physics 2012;39:4013.

74. Noel C, Olsen J, Green OP, et al. TU-G-217A-09: Feasibility of Bowel Tracking Using Onboard Cine MRI for Gated Radiotherapy. Medical Physics 2012;39:3928.

75. Olsen JR, Noel CE, Spencer CR, et al. Feasibility of Single and Multiplane Cine MR for Monitoring Tumor Volumes and Organs-at-Risk (OARs) Position During Radiation Therapy. Int J Radiat Oncol Biol Phys 2012;84:S742.

76. Parikh PJ, Noel CE, Spencer C, et al. Comparison of Onboard Low-field MRI Versus CBCT/MVCT for Anatomy Identification in Radiation Therapy. Int J Radiat Oncol Biol Phys 2012;84:S133.

77. Lagendijk JJW, Raaymakers BW, van Vulpen M. The Magnetic Resonance Imaging–Linac System. Semin Radiat Oncol 2014;24:207-9.

78. Raziee H, Moraes FY, Murgic J, et al. Improved outcomes with dose escalation in localized prostate cancer treated with precision image-guided radiotherapy. Radiother Oncol 2017;123:459-65.

79. de Crevoisier R, Tucker SL, Dong L, et al. Increased risk of biochemical and local failure in patients with distended rectum on the planning CT for prostate cancer radiotherapy. Int J Radiat Oncol Biol Phys 2005;62:965-73.

80. Heemsbergen WD, Hoogeman MS, Witte MG, et al. Increased risk of biochemical and clinical failure for prostate patients with a large rectum at radiotherapy planning: results from the Dutch trial of 68 GY versus 78 Gy. Int J Radiat Oncol Biol Phys 2007;67:1418-24.

81. Kupelian PA, Willoughby TR, Reddy CA, et al. Impact of image guidance on outcomes after external beam radiotherapy for localized prostate cancer. Int J Radiat Oncol Biol Phys 2008;70:1146-50.

82. Singh J, Greer PB, White MA, et al. Treatment-related morbidity in prostate cancer: a comparison of

tau.amegroups.com   *Transl Androl Urol* 2018;7(3):308-320

3-dimensional conformal radiation therapy with and without image guidance using implanted fiducial markers. Int J Radiat Oncol Biol Phys 2013;85:1018-23.

83. Gill S, Thomas J, Fox C, et al. Acute toxicity in prostate cancer patients treated with and without image-guided radiotherapy. Radiat Oncol 2011;6:145.

84. Zelefsky MJ, Kollmeier M, Cox B, et al. Improved clinical outcomes with high-dose image guided radiotherapy compared with non-IGRT for the treatment of clinically localized prostate cancer. Int J Radiat Oncol Biol Phys 2012;84:125-9.

85. Sandler HM, Liu PY, Dunn RL, et al. Reduction in patient-reported acute morbidity in prostate cancer patients treated with 81-Gy Intensity-modulated radiotherapy using reduced planning target volume margins and electromagnetic tracking: assessing the impact of margin

reduction study. Urology 2010;75:1004-8.

86. Sanda MG, Dunn RL, Michalski J, et al. Quality of life and satisfaction with outcome among prostate-cancer survivors. N Engl J Med 2008;358:1250-61.

87. Zelefsky MJ, Levin EJ, Hunt M et al. Incidence of late rectal and urinary toxicities after three-dimensional conformal radiotherapy and intensity-modulated radiotherapy for localized prostate cancer. Int J Radiat Oncol Biol Phys 2008;70:1124-9.

88. Keall PJ, Ng JA, Juneja P, et al. Real-Time 3D Image Guidance Using a Standard LINAC: Measured Motion, Accuracy, and Precision of the First Prospective Clinical Trial of Kilovoltage Intrafraction Monitoring-Guided Gating for Prostate Cancer Radiation Therapy. Int J Radiat Oncol Biol Phys 2016;94:1015-21.

tau.amegroups.com